Implications of 3 + 1 short-baseline neutrino oscillations

Carlo Giunti [a],[*],[1], Marco Laveder [b]

[a] INFN, Sezione di Torino, Via P. Giuria 1, I-10125 Torino, Italy
[b] Dipartimento di Fisica "G. Galilei", Università di Padova, and INFN, Sezione di Padova, Via F. Marzolo 8, I-35131 Padova, Italy

ARTICLE INFO

ABSTRACT

We present an upgrade of the 3 + 1 global fit of short-baseline neutrino oscillation data obtained with the addition of KARMEN and LSND $\nu_e + {}^{12}C \rightarrow {}^{12}N_{g.s.} + e^-$ scattering data. We discuss the implications for the measurements of the effective neutrino mass in β-decay and neutrinoless double-β-decay experiments. We find respective predicted ranges of about 0.1–0.7 eV and 0.01–0.1 eV.

© 2011 Elsevier B.V. All rights reserved.

1. Introduction

The study of active-sterile neutrino oscillations received recently a boost from indications in favor of possible short-baseline oscillations of two types: (1) $\bar{\nu}_\mu \rightarrow \bar{\nu}_e$ oscillations observed in the LSND [1] and MiniBooNE [2] experiments; (2) $\bar{\nu}_e$ and ν_e disappearance revealed, respectively, by the Reactor Anomaly [3] and the Gallium Anomaly [4–10]. In this Letter we consider these indications in the framework of hierarchical 3 + 1 neutrino mixing and we discuss the implications for the measurements of the effective neutrino mass in β-decay and neutrinoless double-β-decay experiments. We also upgrade the global fit presented in Ref. [11] by the addition of KARMEN [12,13] and LSND [14] $\nu_e + {}^{12}C \rightarrow {}^{12}N_{g.s.} + e^-$ scattering data, as suggested in Ref. [15].

Short-baseline (SBL) neutrino oscillations are generated by a squared-mass difference $\Delta m_{SBL}^2 \gtrsim 0.1$ eV^2, which is much larger than the two measured solar (SOL) and atmospheric (ATM) squared-mass differences $\Delta m_{SOL}^2 = (7.6 \pm 0.2) \times 10^{-5}$ eV^2 [16] and $\Delta m_{ATM}^2 = 2.32^{+0.12}_{-0.08} \times 10^{-3}$ eV^2 [17]. The minimal neutrino mixing schemes which can provide a third squared-mass difference for short-baseline neutrino oscillations require the introduction of a sterile neutrino ν_s (see Refs. [18–21]). Hierarchical 3 + 1 neutrino mixing is a perturbation of the standard three-neutrino mixing in which the three active neutrinos ν_e, ν_μ, ν_τ are mainly composed of three massive neutrinos ν_1, ν_2, ν_3 with light masses m_1, m_2, m_3, such that $\Delta m_{SOL}^2 = \Delta m_{21}^2$ and $\Delta m_{ATM}^2 = |\Delta m_{31}^2| \simeq |\Delta m_{32}^2|$, with the standard notation $\Delta m_{kj}^2 \equiv m_k^2 - m_j^2$ (see Ref. [22]). The sterile neu-

trino is mainly composed of a heavy neutrino ν_4 with mass m_4 such that $\Delta m_{SBL}^2 = \Delta m_{41}^2$ and

$$m_1, m_2, m_3 \ll m_4 \quad \Rightarrow \quad m_4 \simeq \sqrt{\Delta m_{41}^2}. \tag{1}$$

Under these hypotheses, the effects of active-sterile neutrino mixing in solar [23,24] and atmospheric [25–28] neutrino experiments are small, but should be revealed sooner or later.

In 3 + 1 neutrino mixing, the effective flavor transition and survival probabilities in short-baseline neutrino oscillation experiments are given by (see Refs. [18–21])

$$P_{\overset{(-)}{\nu_\alpha} \rightarrow \overset{(-)}{\nu_\beta}}^{SBL} = \sin^2 2\vartheta_{\alpha\beta} \sin^2\left(\frac{\Delta m_{41}^2 L}{4E}\right) \quad (\alpha \neq \beta), \tag{2}$$

$$P_{\overset{(-)}{\nu_\alpha} \rightarrow \overset{(-)}{\nu_\alpha}}^{SBL} = 1 - \sin^2 2\vartheta_{\alpha\alpha} \sin^2\left(\frac{\Delta m_{41}^2 L}{4E}\right), \tag{3}$$

for $\alpha, \beta = e, \mu, \tau, s$, with the transition amplitudes

$$\sin^2 2\vartheta_{\alpha\beta} = 4|U_{\alpha 4}|^2 |U_{\beta 4}|^2, \tag{4}$$

$$\sin^2 2\vartheta_{\alpha\alpha} = 4|U_{\alpha 4}|^2 \left(1 - |U_{\alpha 4}|^2\right). \tag{5}$$

The hierarchical 3 + 1 scheme may be compatible with the results of standard cosmological ΛCDM analyses of the Cosmic Microwave Background and Large-Scale Structures data, which constrain the three light neutrino masses to be much smaller than 1 eV [29–32] and indicate that one or two sterile neutrinos may have been thermalized in the early Universe [33–40], with an upper limit of the order of 1 eV on their masses. Also Big-Bang Nucleosynthesis data [41,42] are compatible with the existence of sterile neutrinos, with the indication however that the thermalization of more than one sterile neutrino is disfavored [43,38].

* Corresponding author.
E-mail addresses: giunti@to.infn.it (C. Giunti), laveder@pd.infn.it (M. Laveder).
[1] Also at Department of Theoretical Physics, University of Torino, Italy.

Table 1

Values of χ^2, number of degrees of freedom (NDF), goodness-of-fit (GoF) and best-fit values of the $3+1$ oscillation parameters obtained from the fits of Gallium (GAL), Reactor (REA), $\nu_e + {}^{12}$ C (CAR) data, their combined fit (RGC) and the global fit with (GLO-LOW) and without (GLO-HIG) the MiniBooNE electron neutrino and antineutrino data with reconstructed neutrino energy smaller than 475 MeV. The first three lines correspond to the case of no oscillations (No Osc.). The following nine lines correspond to the case of $3+1$ mixing. The last three lines give the parameter goodness-of-fit (PG) [44].

		REA	GAL	CAR	RGC	GLO-LOW	GLO-HIG
No Osc.	$\chi^2_{\min}$	27.1	12.0	8.2	47.3	195.1	178.1
	NDF	38	4	10	52	144	138
	GoF	0.91	0.017	0.61	0.66	0.0049	0.019
$3+1$	$\chi^2_{\min}$	21.7	2.3	4.6	36.2	152.4	137.5
	NDF	36	2	8	50	144	138
	GoF	97%	32%	80%	93%	30%	50%
	Δm^2_{41} [eV^2]	1.95	2.24	13.80	7.59	0.9	1.6
	$\lvert U_{e4}\rvert^2$	0.026	0.15	0.13	0.036	0.027	0.036
	$\lvert U_{\mu4}\rvert^2$					0.021	0.0084
	$\sin^2 2\vartheta_{e\mu}$					0.0023	0.0012
	$\sin^2 2\vartheta_{ee}$	0.10	0.51	0.45	0.14	0.10	0.14
	$\sin^2 2\vartheta_{\mu\mu}$					0.083	0.034
PG	$\Delta\chi^2_{\min}$				7.6	18.8	11.6
	NDF				4	2	2
	GoF				11%	0.008%	0.3%

The global fit presented in this Letter upgrades that presented in Ref. [11] by the addition of $\nu_e + {}^{12}$ C $\to {}^{12}$ N$_{\mathrm{g.s.}} + e^-$ scattering data, as suggested in Ref. [15]. The considered sets of data are:

- The short-baseline $\overset{(-)}{\nu_\mu} \to \overset{(-)}{\nu_e}$ data of the LSND [1], KARMEN [45], NOMAD [46] and MiniBooNE neutrino [47] and antineutrino [2,48,49] experiments.
- The short-baseline $\bar{\nu}_e$ disappearance data of the Bugey-3 [50], Bugey-4 [51], ROVNO91 [52], Gosgen [53], ILL [54] and Krasnoyarsk [55] reactor antineutrino experiments, taking into account the new calculation of the reactor $\bar{\nu}_e$ flux [56,57] which indicates a small $\bar{\nu}_e$ disappearance (the reactor antineutrino anomaly [3]), and the KamLAND [58] bound on $\lvert U_{e4}\rvert^2$ (see Ref. [59]).
- The short-baseline ν_μ disappearance data of the CDHSW experiment [60], the constraints on $\lvert U_{\mu4}\rvert^2$ obtained in Ref. [61] from the analysis of the data of atmospheric neutrino oscillation experiments, and the bound on $\lvert U_{\mu4}\rvert^2$ obtained from MINOS neutral-current data [62] (see Refs. [63,11]).
- The data of Gallium radioactive source experiments (GALLEX [4–6] and SAGE [7–10]) which indicate a ν_e disappearance (the Gallium neutrino anomaly [64–72,3]). We analyze the Gallium data according to Ref. [72].
- The $\nu_e + {}^{12}$ C $\to {}^{12}$ N$_{\mathrm{g.s.}} + e^-$ scattering data of the KARMEN [12,13] and LSND [14] experiments, which constrain the short-baseline ν_e disappearance [15].

The plan of the Letter is as follows. Since this is the first time that the KARMEN and LSND $\nu_e + {}^{12}$ C $\to {}^{12}$ N$_{\mathrm{g.s.}} + e^-$ scattering data are taken into account in a global fit of neutrino oscillation short-baseline data, in Section 2 we discuss the method of the analysis and we present the ensuing upgrade of the global fit published in Ref. [11]. In Section 3 we discuss the predictions for the effective electron neutrino mass in β-decay. In Section 4 we present the predictions for the effective Majorana neutrino mass in neutrino-less double-β-decay. In Section 5 we draw our conclusions.

2. Global fit

In this section we present the upgrade of the results of the global fit of short-baseline neutrino oscillation data obtained in

Ref. [11] with the inclusion of the KARMEN [12,13] and LSND [14] $\nu_e + {}^{12}$ C $\to {}^{12}$ N$_{\mathrm{g.s.}} + e^-$ scattering data suggested in Ref. [15].

We analyzed the KARMEN and LSND data summarized in Ref. [15] without assuming a theoretical model for the $\nu_e + {}^{12}$ C $\to {}^{12}$ N$_{\mathrm{g.s.}} + e^-$ cross section. We assumed only a dependence of the cross section on $(E - Q)^2$, where $Q = 17.3$ MeV is the Q-value of the reaction. Such dependence on the neutrino energy E is due to the allowed character of the transition from the 0^+ ground state of ^{12}C to the 1^+ ground state of ^{12}N. The information on neutrino oscillations comes from the different source-detector distances in KARMEN and LSND: $L_{\mathrm{KARMEN}} = 17.7$ m and $L_{\mathrm{LSND}} = 29.8$ m. The best fit values of the oscillation parameters and the 95% C.L. allowed region in the $\sin^2 2\vartheta_{ee}$–Δm^2_{41} plane are given, respectively, in Table 1 and Fig. 1, together with the corresponding quantities obtained from the analysis of reactor and Gallium data.

The $\nu_e - {}^{12}$ C curve in Fig. 1 is an exclusion curve which proscribes the region of the oscillation parameters on the right. The best-fit is obtained for rather large values of the oscillation parameters: $\Delta m^2_{41} = 13.80$ eV^2 and $\sin^2 2\vartheta_{ee} = 0.45$. The reason of the improvement of the value of $\chi^2_{\min}$ obtained with the best-fit values of the oscillation parameters with respect to the case of no oscillations can be understood from Fig. 2, where one can see that there is an improvement in the fit of the KARMEN data due to the shorter source-detector distance with respect to the LSND data, for which there is practically no improvement, because oscillations are averaged out. From Fig. 1 one can see that for $\Delta m^2_{41} \gtrsim 20$ eV^2 there is no constraint on neutrino oscillations from $\nu_e - {}^{12}$ C because the oscillations are averaged out in both the KARMEN and LSND experiments.

The comparison of the 95% C.L. reactor, Gallium and $\nu_e - {}^{12}$ C allowed regions in the $\sin^2 2\vartheta_{ee}$–Δm^2_{41} plane presented in Fig. 1 shows that there is a region of overlap for $0.1 \lesssim \sin^2 2\vartheta_{ee} \lesssim 0.2$ and $\Delta m^2_{41} \gtrsim 2$ eV^2, indicating that the results of the three sets of data are compatible with the hypothesis of neutrino oscillations.

Fig. 1 shows also the 95% C.L. allowed region in the $\sin^2 2\vartheta_{ee}$–Δm^2_{41} plane obtained from the combined analysis of reactor, Gallium and $\nu_e - {}^{12}$ C, with the best-fit values of the oscillation parameters listed in Table 1. The compatibility of the three sets of data is confirmed by the 11% value of the parameter goodness-of-fit [44].
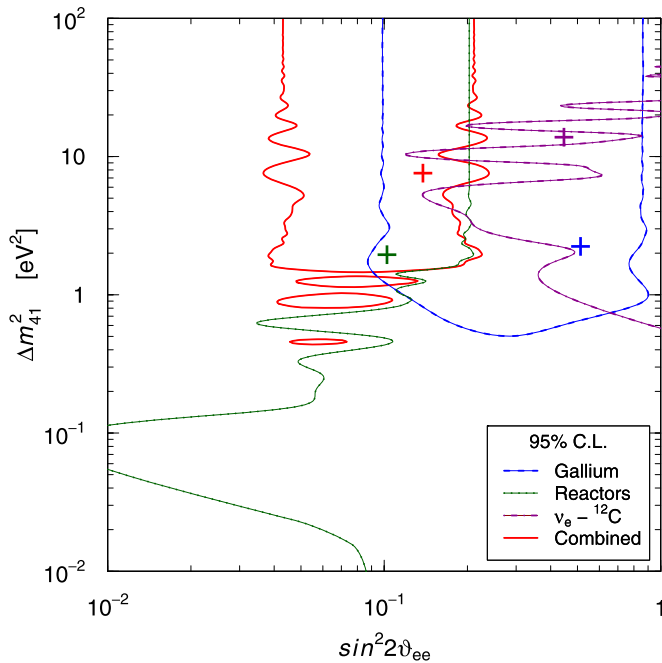
Fig. 1. Superposition of the 95% C.L. contours in the $\sin^2 2\vartheta_{ee}$–Δm_{41}^2 plane obtained from the separate fits of Gallium, reactor and $\nu_e - {}^{12}C$ data and that obtained from the combined fit. The best-fit points are indicated by crosses (see Table 1).
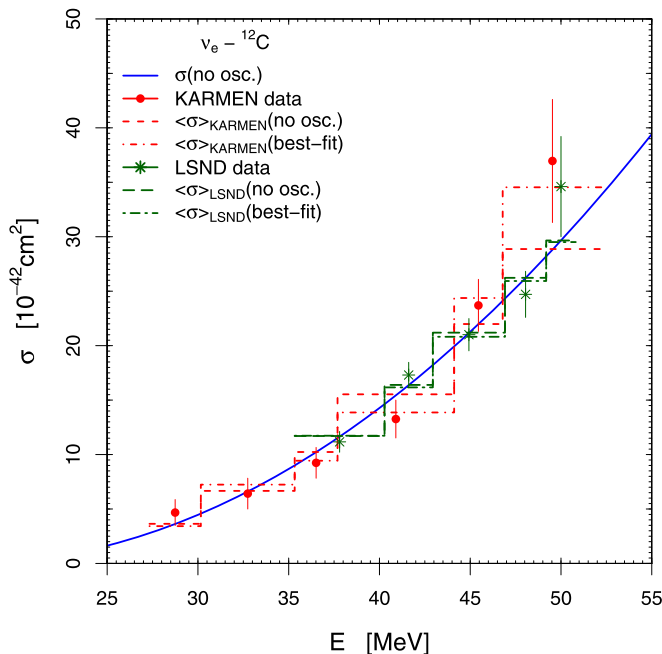
Fig. 2. KARMEN and LSND $\nu_e - {}^{12}C$ cross section data (points and asterisks, respectively) with the corresponding statistical error bars. The solid blue line shows the best-fit dependence of the cross section on the neutrino energy E in the case of no oscillations. The dashed red and long-dashed green histograms show, respectively, the corresponding average cross section for the energy bins of the KARMEN and LSND data. The dash-dotted red and long-dash-dotted green histograms show, respectively, the average cross section modulated by the best-fit oscillation probability for the energy bins of the KARMEN and LSND data. (For interpretation of the references to colour in this figure legend, the reader is referred to the web version of this Letter.)

Fig. 3 shows the allowed regions in the $\sin^2 2\vartheta_{e\mu}$–Δm_{41}^2, $\sin^2 2\vartheta_{ee}$–Δm_{41}^2 and $\sin^2 2\vartheta_{\mu\mu}$–$\Delta m_{41}^2$ planes obtained from the global analysis of short-baseline neutrino oscillation data listed in the Introduction. We made two global analyses named GLO-LOW

and GLO-HIG, respectively, with and without the three MiniBooNE electron neutrino and antineutrino bins with reconstructed neutrino energy smaller than 475 MeV, which have an excess of events called the "MiniBooNE low-energy anomaly". The best-fit values of the oscillation parameters are listed in Table 1. In the global analyses we consider values of Δm_{41}^2 smaller than 10 eV^2, since larger values are strongly incompatible with the cosmological constraints on neutrino masses [33–40].

The GLO-LOW and GLO-HIG analyses are similar, respectively, to the LOW-GAL and HIG-GAL analyses presented in Ref. [11], but take into account in addition the KARMEN and LSND $\nu_e - {}^{12}C$ scattering data. From Fig. 3 and Table 1 one can see that the contribution of the $\nu_e - {}^{12}C$ data is beneficial for the lowering of the best-fit value of Δm_{41}^2 from 5.6 eV^2 obtained in Ref. [11] to 0.9 eV^2 in GLO-LOW and 1.6 eV^2 in GLO-HIG. These values of Δm_{41}^2 are more compatible with the cosmological constraints on neutrino masses [33–40].

Comparing the GLO-LOW and GLO-HIG parts of Fig. 3 and Table 1 one can see that the inclusion of the fit of the MiniBooNE low-energy data favors small values of Δm_{41}^2. This fact has been noted and explained in Ref. [11]. Hence, the results of the GLO-LOW analysis are more attractive than those of the GLO-HIG in view of a better compatibility with cosmological constraints on the neutrino masses.

The well-known tension between appearance and disappearance data [73–76,19,77,61,78,79,78,59,80,81,11,82] is slightly worsened by the inclusion in the fit of the $\nu_e - {}^{12}C$ scattering data, which strengthen the disappearance constrain.

In the GLO-LOW analysis the 0.008% parameter goodness-of-fit, has worsened with respect to the 0.04% obtained in Ref. [11], which was already so low that we wrote that the MiniBooNE low-energy anomaly "may have an explanation different from $\overset{(-)}{\nu_\mu} \to \overset{(-)}{\nu_e}$ oscillations". Nevertheless, in the following we will discuss the GLO-LOW predictions on the effective neutrino masses measured in β-decay and neutrinoless double-β-decay experiments, because we are not aware of an a-priori argument which allows to exclude from the analysis the MiniBooNE low-energy data. The exclusion a-posteriori motivated by the results of the fit may be hazardous, taking also into account the nice value of the global goodness-of-fit (30%) and the above-mentioned preference for small values of Δm_{41}^2 in agreement with the same preference of the cosmological data.

Considering the GLO-HIG analysis, the 0.3% appearance–disappearance parameter goodness-of-fit is lower than that obtained in Ref. [11] (1%) because of the above-mentioned strengthening of the disappearance constraint induced by the $\nu_e - {}^{12}C$ scattering data. However, the appearance–disappearance parameter goodness-of-fit is not dramatically low and the fit cannot be rejected, also taking into account the pleasant 50% value of the global goodness-of-fit.

In the next two sections we discuss the predictions for the effective neutrino masses measured in β-decay and neutrinoless double-β-decay experiments.

3. β-Decay

The effective electron neutrino mass m_β in β-decay experiments is given by [83–86] (other approaches are discussed in Refs. [87–89])

$$m_\beta^2 = \sum_k |U_{ek}|^2 m_k^2. \tag{6}$$

The most accurate measurements of m_β have been obtained in the Mainz [90] and Troitsk [91] experiments, whose combined upper
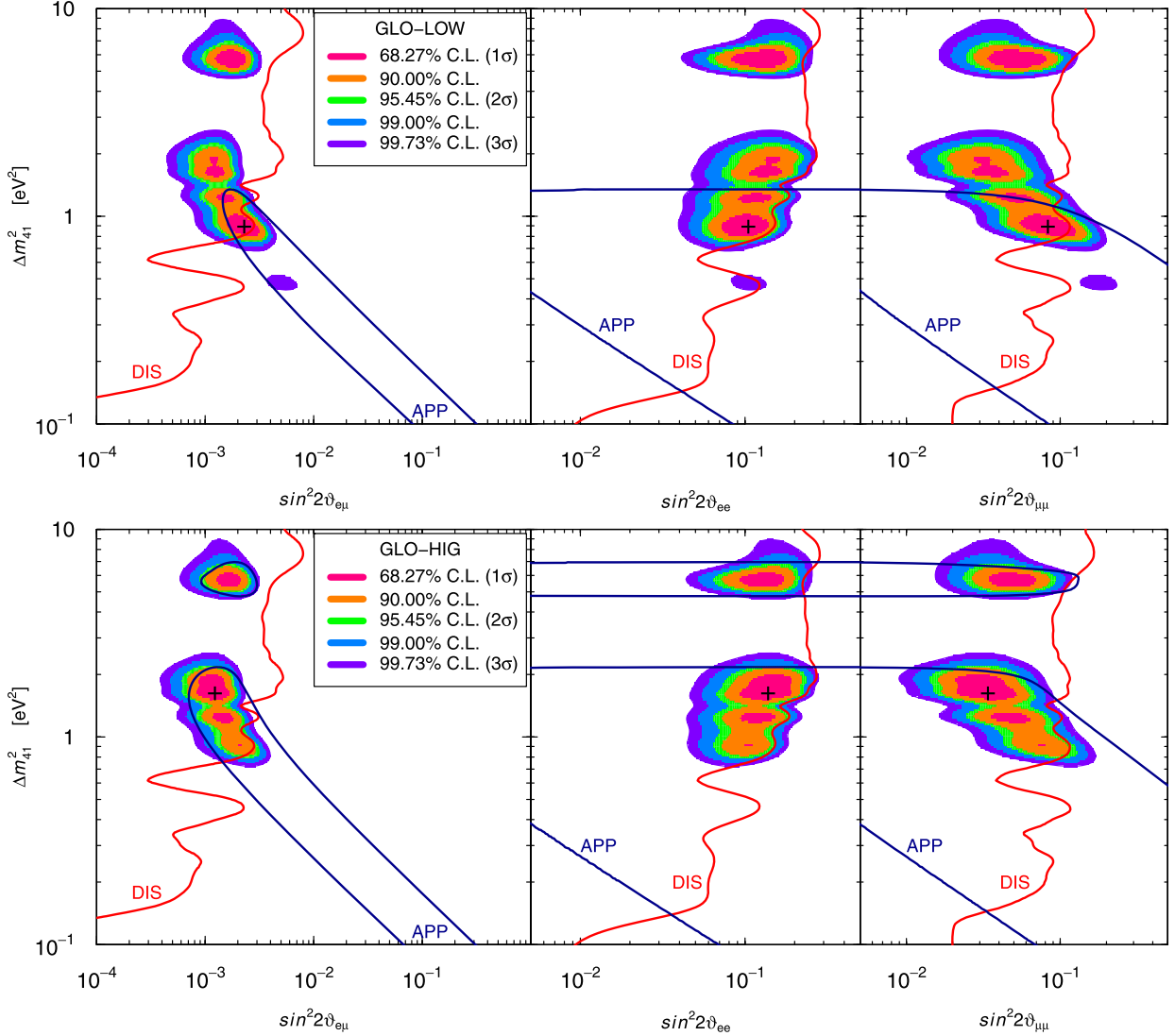
Fig. 3. Allowed regions in the $\sin^2 2\vartheta_{e\mu} - \Delta m^2_{41}$, $\sin^2 2\vartheta_{ee} - \Delta m^2_{41}$ and $\sin^2 2\vartheta_{\mu\mu} - \Delta m^2_{41}$ planes obtained from the GLO-LOW and GLO-HIG global analyses of short-baseline neutrino oscillation data (see Table 1). The best-fit points are indicated by crosses (see Table 1). The thick solid blue lines with the label APP show the 3σ allowed regions obtained from the analysis of $\overset{(-)}{\nu_\mu} \to \overset{(-)}{\nu_e}$ appearance data. The thick solid red lines with the label DIS show the 3σ allowed regions obtained from the analysis of disappearance data. (For interpretation of the references to colour in this figure legend, the reader is referred to the web version of this Letter.)

bound is [70]

$$m_\beta \leqslant 1.8 \text{ eV} \quad (\text{Mainz} + \text{Troitsk, 95\% C.L.}). \tag{7}$$

In the hierarchical $3 + 1$ scheme we have the lower bound

$$m_\beta \geqslant |U_{e4}|\sqrt{\Delta m^2_{41}} \equiv m^{(4)}_\beta. \tag{8}$$

Therefore, from the analysis of short-baseline neutrino oscillation data we can derive predictions for the possibility of observing a neutrino mass effect in the KATRIN experiment [92], which is under construction and scheduled to start in 2012, and in other possible future experiments.

Let us however note that the effective electron neutrino mass in Eq. (6) has been derived assuming that all the neutrino masses are smaller than the experimental energy resolution (see Ref. [22]). If m_4 is of the order of 1 eV, the approximation is acceptable for the interpretation of the result of the Mainz and Troitsk experiments, which had, respectively, energy resolutions of 4.8 eV and 3.5 eV [93]. On the other hand, the energy resolution of the KATRIN experiment will be 0.93 eV near the end-point of the en-

ergy spectrum of the electron emitted in Tritium decay, at $T = Q$, where T is the kinetic energy of the electron and $Q = 18.574$ keV is the Q-value of the decay. If the value of m_4 is larger than the energy resolution of the experiment, its effect on the measured electron spectrum cannot be summarized by one effective quantity, because the Kurie function $K(T)$ is given by
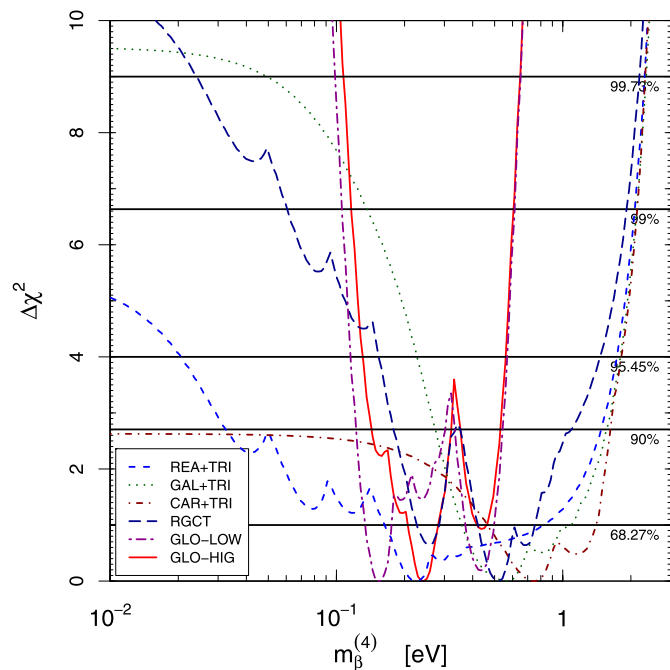
$$\frac{K^2(T)}{Q - T} = \sqrt{(Q - T)^2 - \widetilde{m}^2_\beta} - |U_{e4}|^2(Q - T)$$
$$+ |U_{e4}|^2 \sqrt{(Q - T)^2 - m^2_4}\, \theta(Q - T - m_4), \tag{9}$$

where $\widetilde{m}^2_\beta = \sum^3_{k=1} |U_{ek}|^2 m^2_k$ is the contribution of the three neutrino masses much smaller than 1 eV and θ is the Heaviside step function.

In the following we discuss the predictions obtained from the GLO-LOW and GLO-HIG analyses of short-baseline neutrino oscillation data for both the contribution $m^{(4)}_\beta$ to the effective mass in β-decay and the distortion of the Kurie function due to m_4.

Table 2

Allowed 1σ, 2σ and 3σ ranges of $m_4 = \sqrt{\Delta m_{41}^2}$, $|U_{e4}|^2$, $m_\beta^{(4)} = |U_{e4}|\sqrt{\Delta m_{41}^2}$ and $m_{\beta\beta}^{(4)} = |U_{e4}|^2\sqrt{\Delta m_{41}^2}$ obtained from the fits of Tritium data with Gallium (GAL+TRI), Reactor (REA+TRI) and $\nu_e - {}^{12}$C (CAR+TRI) data, their combined fit (RGCT) and the global fit with (GLO-LOW) and without (GLO-HIG) the MiniBooNE electron neutrino and antineutrino data with reconstructed neutrino energy smaller than 475 MeV. Masses are given in eV.

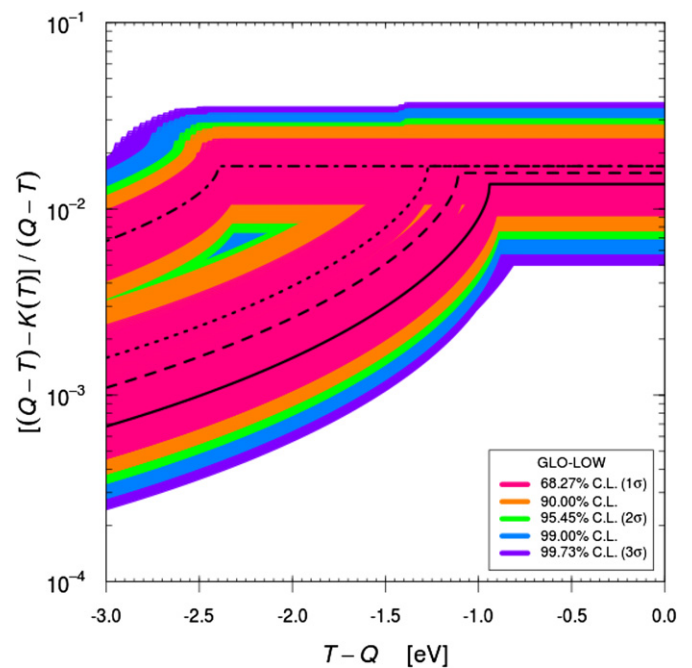|	REA+TRI	GAL+TRI	CAR+TRI	RGCT	GLO-LOW	GLO-HIG
m_4	1.3–5.2	1.0–2.8	2.7–3.8	1.4–3.8	0.91–2.5	1.2–2.4
	0.41–13	0.85–5.2	< 245	1.2–8.4	0.88–2.5	0.91–2.5
	< 343	0.22–11	< 412	0.42–16	0.85–2.8	0.87–2.8
$|U_{e4}|^2$	0.01–0.04	0.09–0.20	0.03–0.14	0.02–0.05	0.02–0.04	0.03–0.05
	0.00–0.05	0.04–0.28	–	0.01–0.06	0.02–0.06	0.02–0.06
	< 0.06	> 0.00	–	0.00–0.07	0.01–0.07	0.01–0.07
$m_\beta^{(4)}$	0.16–0.81	0.36–1.06	0.48–1.40	0.23–0.74	0.14–0.49	0.21–0.45
	0.02–1.69	0.23–1.79	< 1.79	0.15–1.45	0.12–0.56	0.13–0.56
	< 2.29	0.05–2.29	< 2.29	0.02–2.15	0.10–0.65	0.11–0.63
$m_{\beta\beta}^{(4)}$	0.021–0.13	0.110–0.41	0.081–0.51	0.039–0.15	0.020–0.10	0.035–0.09
	< 0.30	0.048–0.76	< 0.78	0.019–0.28	0.015–0.13	0.018–0.12
	< 0.42	0.003–1.03	< 1.17	0.001–0.44	0.011–0.16	0.013–0.16

Fig. 4. Marginal $\Delta\chi^2 = \chi^2 - \chi^2_{\min}$ as a function of the contribution $m_\beta^{(4)} = |U_{e4}|\sqrt{\Delta m_{41}^2}$ to the effective β-decay electron-neutrino mass m_β obtained from the fits of Tritium (TRI) data with Reactor (REA), Gallium (GAL) and $\nu_e - {}^{12}$C (CAR) data, their combined fit (RGCT) and the GLO-LOW and GLO-HIG global fits.

Fig. 5. Bands of the relative deviation of the Kurie plot in β-decay corresponding to the allowed regions in the $\sin^2 2\vartheta_{ee}-\Delta m_{41}^2$ plane in Fig. 3, obtained from the GLO-LOW global analysis of short-baseline neutrino oscillation data (see Table 1). The black solid line corresponds to the best-fit point ($m_4 = 0.94$ eV and $|U_{e4}|^2 = 0.027$). The dashed, dotted and dash-dotted lines correspond, respectively, to the local minima at ($m_4 = 1.11$ eV, $|U_{e4}|^2 = 0.03$), ($m_4 = 1.27$ eV, $|U_{e4}|^2 = 0.035$) and ($m_4 = 2.40$ eV, $|U_{e4}|^2 = 0.033$).

Fig. 4 shows the marginal $\Delta\chi^2 = \chi^2 - \chi^2_{\min}$ as a function of $m_\beta^{(4)}$ for the data analyses listed in Table 2, which gives the 1σ, 2σ and 3σ allowed ranges of m_4, $|U_{e4}|^2$ and $m_\beta^{(4)}$.

The predictions for $m_\beta^{(4)}$ obtained from the analyses of reactor, Gallium and $\nu_e - {}^{12}$C data are interesting, because these data give direct information on $|U_{e4}|$ from the amplitude of $\overset{(-)}{\nu}_e$ disappearance (see Eq. (5)). Since the data of these experiments do not allow us to constrain the upper value of Δm_{41}^2, as can be seen in Fig. 1, we have analyzed their data in combination with the Tritium data of the Mainz [90] and Troitsk [91] experiment. This is the origin of the corresponding upper limits for m_4 and $m_\beta^{(4)}$ in Table 2 and the corresponding steep rise of $\Delta\chi^2$ for $m_\beta^{(4)} \gtrsim 2$ eV in Fig. 4.

As one can see from Fig. 4 and Table 2, the most stringent predicted ranges for $m_\beta^{(4)}$ are obtained in the GLO-LOW and GLO-

HIG analyses, but all the analyses agree in favoring values of $m_\beta^{(4)}$ between about 0.1 and 0.7 eV, which is promising for the perspectives of future experiments.

In Figs. 5 and 6 we show the relative deviation of the Kurie function from the massless case ($K(T) = Q - T$) obtained in the GLO-LOW and GLO-HIG analyses, neglecting the contribution of $\widetilde{m}_\beta$ in Eq. (9). For $T > Q - m_4$ the deviation is constant, because the Kurie function in Eq. (9) reduces to

$$K(T) = (Q - T)\sqrt{1 - |U_{e4}|^2}. \tag{10}$$

For $T = Q - m_4$ there is a kink and for $T < Q - m_4$ the Kurie function depends on both m_4 and $|U_{e4}|^2$, as given by Eq. (9).

From Figs. 5 and 6 one can see that high precision will be needed in order to see the effect of m_4 and measure $|U_{e4}|^2$,
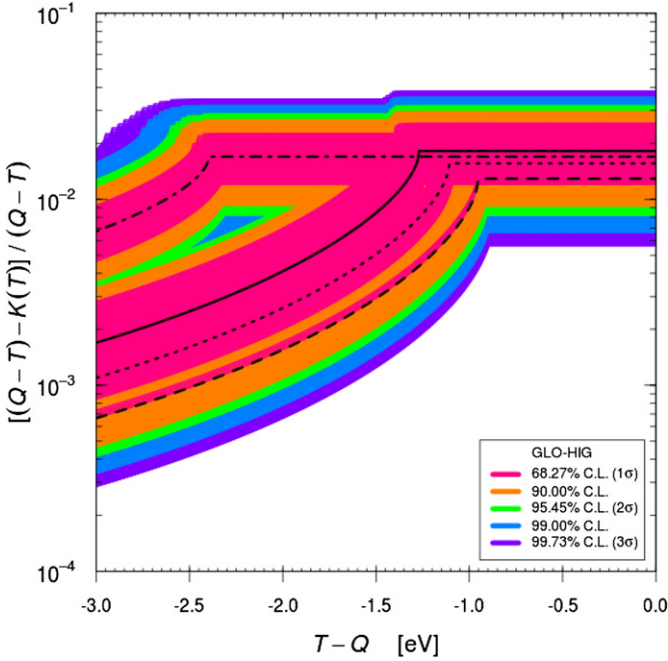
Fig. 6. Bands of the relative deviation of the Kurie plot in β-decay corresponding to the allowed regions in the $\sin^2 2\vartheta_{ee}$–Δm_{41}^2 plane in Fig. 3, obtained from the GLO-HIG global analysis of short-baseline neutrino oscillation data (see Table 1). The black solid line corresponds to the best-fit point ($m_4 = 1.27$ eV and $|U_{e4}|^2 = 0.036$). The dashed, dotted and dash-dotted lines correspond, respectively, to the local minima at ($m_4 = 0.95$ eV, $|U_{e4}|^2 = 0.027$), ($m_4 = 1.11$ eV, $|U_{e4}|^2 = 0.031$) and ($m_4 = 2.40$ eV, $|U_{e4}|^2 = 0.033$).

which is the only parameter which determines the deviation of $K(T)$ from the massless Kurie function near the end point, for $T > Q - m_4$. If the mixing parameters are near the best-fit point of the GLO-LOW analysis, a precision of about one percent will be needed within 1 eV from the end-point of the spectrum. Finding the effect of m_4 farther from the end-point, for $T < Q - m_4$ is more difficult, because the relative deviation of the Kurie function can be as small as about 10^{-3}. The GLO-HIG analysis prefers slightly larger values of m_4, but the discovery of an effect in β-decay will require a similar precision.
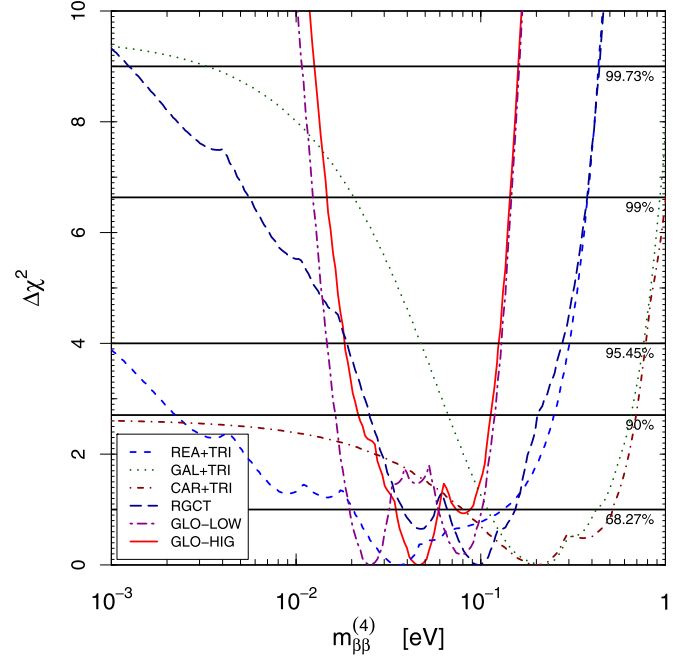
4. Neutrinoless $\beta\beta$-decay

If massive neutrinos are Majorana particles, neutrinoless double-β decay is possible, with a decay rate proportional to the effective Majorana mass (see Refs. [94–98,22])

$$m_{\beta\beta} = \left| \sum_k U_{ek}^2 m_k \right|. \tag{11}$$

The results of the analysis of short-baseline oscillation data allow us to calculate the contribution of the heaviest massive neutrino ν_4 to $m_{\beta\beta}$, which is given by

$$m_{\beta\beta}^{(4)} = |U_{e4}|^2 \sqrt{\Delta m_{41}^2}, \tag{12}$$

taking into account the mass hierarchy in Eq. (1). If there are no unlikely cancellations among the contributions of m_1, m_2, m_3 and that of m_4 [99] (possible cancellations are discussed in Refs. [100, 101]), the value of $m_{\beta\beta}^{(4)}$ is a lower bound for the effective neutrino mass which could be observed in future neutrinoless double-β decay experiments (see the review in Ref. [102]).

Fig. 7. Marginal $\Delta\chi^2 = \chi^2 - \chi_{\min}^2$ as a function of the contribution $m_{\beta\beta}^{(4)} = |U_{e4}|^2 \sqrt{\Delta m_{41}^2}$ to the effective neutrinoless double-β decay Majorana mass $m_{\beta\beta}$ obtained from the fits of Tritium (TRI) data with Reactor (REA), Gallium (GAL) and $\nu_e - {}^{12}$C (CAR) data, their combined fit (RGCT) and the GLO-LOW and GLO-HIG global fits.

Fig. 7 shows the marginal $\Delta\chi^2$ as a function of $m_{\beta\beta}^{(4)}$ for the data analyses listed in Table 2, which gives the 1σ, 2σ and 3σ allowed ranges of $m_{\beta\beta}^{(4)}$.

The analyses of the Gallium and $\nu_e - {}^{12}$C scattering data give optimistic indications in favor of a value of $m_{\beta\beta}^{(4)}$ of about 0.2 eV, albeit with large uncertainties, but their combined fit with reactor data lowers the prediction to a best-fit value of about 0.1 eV, with a 1σ allowed range which extends down to about 0.04 eV. The reason is that reactor data constrain $|U_{e4}|^2$ to small values, as can be seen in Table 2.

The predictions for $m_{\beta\beta}^{(4)}$ obtained from global GLO-LOW and GLO-HIG agree in indicating a 3σ allowed range between about 0.01 and 0.1 eV. The connection of the value of $m_{\beta\beta}^{(4)}$ with the allowed regions for the oscillation parameters is clarified in Figs. 8 and 9, where we show the allowed regions in the $|U_{e4}|^2$–m_4 plane obtained, respectively, from the GLO-LOW and GLOW-HIG analyses, together with lines of constant $m_{\beta\beta}^{(4)}$. One can see that if the oscillation parameters are close to the best-fit point of the GLO-LOW analysis, at $m_4 = 0.94$ eV, which is favored by cosmological data, the value of $m_{\beta\beta}^{(4)}$ is about 0.02–0.03 eV. In order to have a large value of $m_{\beta\beta}^{(4)}$, around 0.1 eV, the oscillation parameters must lie in the large-m_4 region at $m_4 \simeq 2.40$ eV, or on the large-$|U_{e4}|^2$ border of the allowed region at $m_4 \simeq 1.27$ eV.

5. Conclusions

In this Letter we presented an upgrade of the $3 + 1$ global fit of short-baseline neutrino oscillation data presented in Ref. [11] obtained with the addition of KARMEN [12,13] and LSND [14] $\nu_e + {}^{12}$C $\rightarrow {}^{12}$N$_{g.s.} + e^-$ scattering data, as suggested in Ref. [15]. We have shown that the new data favor low values of Δm_{41}^2, which are appealing in view of the cosmological constraints on neutrino masses [33–40].
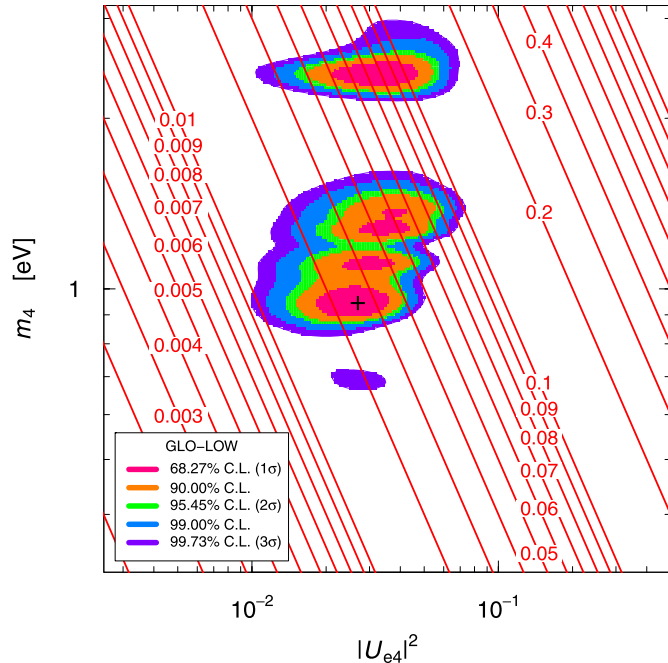
Fig. 8. Allowed regions in the $|U_{e4}|^2$–m_4 plane obtained from the GLO-LOW global analysis of short-baseline neutrino oscillation data (see Table 1). The best-fit point is indicated by a cross (see Table 1). The red lines have the indicated constant value of $m_{\beta\beta}^{(4)} = |U_{e4}|^2 \sqrt{\Delta m_{41}^2}$. (For interpretation of the references to colour in this figure legend, the reader is referred to the web version of this Letter.)
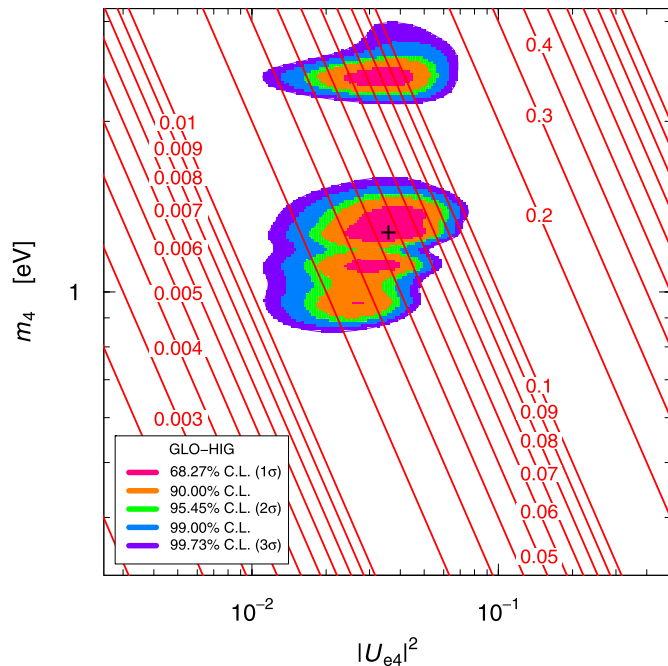
Fig. 9. Allowed regions in the $|U_{e4}|^2$–m_4 plane obtained from the GLO-HIG global analysis of short-baseline neutrino oscillation data (see Table 1). The best-fit point is indicated by a cross (see Table 1). The red lines have the indicated constant value of $m_{\beta\beta}^{(4)} = |U_{e4}|^2 \sqrt{\Delta m_{41}^2}$. (For interpretation of the references to colour in this figure legend, the reader is referred to the web version of this Letter.)

We discussed the implications for the measurements of the effective neutrino mass in β-decay and neutrinoless double-β-decay experiments.

The predicted contribution of m_4 to the effective neutrino mass m_β in β-decay is in the range between about 0.1 and 0.7 eV, most

of which will be explored after 2012 by the KATRIN experiment [92], which will have a sensitivity of about 0.2 eV. If KATRIN or future experiments will have a precision of about one percent near the end-point of the spectrum, for $T > Q - m_4$, the effects of m_4 and $|U_{e4}|^2$ may be measured separately.

The predicted contribution of m_4 to the effective Majorana mass $m_{\beta\beta}$ in neutrinoless double-β decay is in the range between about 0.01 and 0.1 eV. The expected value of $m_{\beta\beta}$ is smaller than the expected value of m_β because it is suppressed by an additional power of $|U_{e4}|$, which is small. Nevertheless, it is important that $m_{\beta\beta}$ has a lower limit (if no unlikely cancellations among the four mass contributions occur [99]) which is an important motivation for the development of neutrinoless double-β decay experiments [102].

Acknowledgement

References

[1] A. Aguilar, et al., LSND, Phys. Rev. D 64 (2001) 112007, hep-ex/0104049.
[2] A.A. Aguilar-Arevalo, et al., MiniBooNE, Phys. Rev. Lett. 105 (2010) 181801, arXiv:1007.1150.
[3] G. Mention, et al., Phys. Rev. D 83 (2011) 073006, arXiv:1101.2755.
[4] P. Anselmann, et al., GALLEX, Phys. Lett. B 342 (1995) 440.
[5] W. Hampel, et al., GALLEX, Phys. Lett. B 420 (1998) 114.
[6] F. Kaether, W. Hampel, G. Heusser, J. Kiko, T. Kirsten, Phys. Lett. B 685 (2010) 47, arXiv:1001.2731.
[7] J.N. Abdurashitov, et al., SAGE, Phys. Rev. Lett. 77 (1996) 4708.
[8] J.N. Abdurashitov, et al., SAGE, Phys. Rev. C 59 (1999) 2246, hep-ph/9803418.
[9] J.N. Abdurashitov, et al., SAGE, Phys. Rev. C 73 (2006) 045805, nucl-ex/0512041.
[10] J.N. Abdurashitov, et al., SAGE, Phys. Rev. C 80 (2009) 015807, arXiv:0901.2200.
[11] C. Giunti, M. Laveder, arXiv:1109.4033, 2011.
[12] B.E. Bodmann, et al., KARMEN, Phys. Lett. B 332 (1994) 251.
[13] B. Armbruster, et al., Phys. Rev. C 57 (1998) 3414, hep-ex/9801007.
[14] L.B. Auerbach, et al., LSND, Phys. Rev. C 64 (2001) 065501, hep-ex/0105068.
[15] J. Conrad, M. Shaevitz, arXiv:1106.5552, 2011.
[16] K. Abe, et al., Super-Kamiokande, Phys. Rev. D 83 (2011) 052010, arXiv:1010.0118.
[17] P. Adamson, et al., MINOS, Phys. Rev. Lett. 106 (2011) 181801, arXiv:1103.0340.
[18] S.M. Bilenky, C. Giunti, W. Grimus, Prog. Part. Nucl. Phys. 43 (1999) 1, hep-ph/9812360.
[19] M. Maltoni, T. Schwetz, M. Tortola, J. Valle, New J. Phys. 6 (2004) 122, hep-ph/0405172.
[20] A. Strumia, F. Vissani, hep-ph/0606054, 2006.
[21] M.C. Gonzalez-Garcia, M. Maltoni, Phys. Rept. 460 (2008) 1, arXiv:0704.1800.
[22] C. Giunti, C.W. Kim, Fundamentals of Neutrino Physics and Astrophysics, Oxford University Press, Oxford, UK, 2007.
[23] C. Giunti, Y. Li, Phys. Rev. D 80 (2009) 113007, arXiv:0910.5856.
[24] A. Palazzo, Phys. Rev. D 83 (2011) 113013, arXiv:1105.1705.
[25] S. Choubey, JHEP 0712 (2007) 014, arXiv:0709.1937.
[26] S. Razzaque, A.Y. Smirnov, JHEP 1107 (2011) 084, arXiv:1104.1390.
[27] R. Gandhi, P. Ghoshal, arXiv:1108.4360, 2011.
[28] V. Barger, Y. Gao, D. Marfatia, arXiv:1109.5748, 2011.
[29] G.L. Fogli, et al., Phys. Rev. D 78 (2008) 033010, arXiv:0805.2517.
[30] B.A. Reid, L. Verde, R. Jimenez, O. Mena, JCAP 1001 (2010) 003, arXiv:0910.0008.
[31] S.A. Thomas, F.B. Abdalla, O. Lahav, Phys. Rev. Lett. 105 (2010) 031301, arXiv:0911.5291.
[32] M.C. Gonzalez-Garcia, M. Maltoni, J. Salvado, JHEP 1008 (2010) 117, arXiv:1006.3795.
[33] J. Hamann, S. Hannestad, G.G. Raffelt, I. Tamborra, Y.Y. Wong, Phys. Rev. Lett. 105 (2010) 181301, arXiv:1006.5276.
[34] E. Giusarma, et al., Phys. Rev. D 83 (2011) 115023, arXiv:1102.4774.
[35] J.R. Kristiansen, O. Elgaroy, arXiv:1104.0704, 2011.
[36] Z. Hou, R. Keisler, L. Knox, M. Millea, C. Reichardt, arXiv:1104.2333, 2011.
[37] A.X. Gonzalez-Morales, R. Poltis, B.D. Sherwin, L. Verde, arXiv:1106.5052, 2011.
[38] J. Hamann, S. Hannestad, G.G. Raffelt, Y.Y. Wong, JCAP 1109 (2011) 034, arXiv:1108.4136.
[39] M. Archidiacono, E. Calabrese, A. Melchiorri, arXiv:1109.2767, 2011.
[40] J. Hamann, arXiv:1110.4271, 2011.

[41] R.H. Cyburt, B.D. Fields, K.A. Olive, E. Skillman, Astropart. Phys. 23 (2005) 313, astro-ph/0408033.
[42] Y.I. Izotov, T.X. Thuan, Astrophys. J. 710 (2010) L67, arXiv:1001.4440.
[43] G. Mangano, P.D. Serpico, Phys. Lett. B 701 (2011) 296, arXiv:1103.1261.
[44] M. Maltoni, T. Schwetz, Phys. Rev. D 68 (2003) 033020, hep-ph/0304176.
[45] B. Armbruster, et al., KARMEN, Phys. Rev. D 65 (2002) 112001, hep-ex/0203021.
[46] P. Astier, et al., NOMAD, Phys. Lett. B 570 (2003) 19, hep-ex/0306037.
[47] A.A. Aguilar-Arevalo, MiniBooNE, Phys. Rev. Lett. 102 (2009) 101802, arXiv:0812.2243.
[48] E. Zimmerman, MiniBooNE, PANIC 2011 (2011).
[49] Z. Djurcic, MiniBooNE, NUFACT 2011 (2011).
[50] B. Achkar, et al., Bugey, Nucl. Phys. B 434 (1995) 503.
[51] Y. Declais, et al., Bugey, Phys. Lett. B 338 (1994) 383.
[52] A. Kuvshinnikov, L. Mikaelyan, S. Nikolaev, M. Skorokhvatov, A. Etenko, JETP Lett. 54 (1991) 253.
[53] G. Zacek, et al., CalTech-SIN-TUM, Phys. Rev. D 34 (1986) 2621.
[54] A. Hoummada, S. Lazrak Mikou, G. Bagieu, J. Cavaignac, D. Holm Koang, Appl. Rad. Isot. 46 (1995) 449.
[55] G.S. Vidyakin, et al., Sov. Phys. JETP 71 (1990) 424.
[56] T.A. Mueller, et al., Phys. Rev. C 83 (2011) 054615, arXiv:1101.2663.
[57] P. Huber, Phys. Rev. C 84 (2011) 024617, arXiv:1106.0687.
[58] S. Abe, et al., KamLAND, Phys. Rev. Lett. 100 (2008) 221803, arXiv:0801.4589.
[59] C. Giunti, M. Laveder, Phys. Rev. D 83 (2011) 053006, arXiv:1012.0267.
[60] F. Dydak, et al., CDHSW, Phys. Lett. B 134 (1984) 281.
[61] M. Maltoni, T. Schwetz, Phys. Rev. D 76 (2007) 093005, arXiv:0705.0107.
[62] P. Adamson, et al., MINOS, Phys. Rev. Lett. 107 (2011) 011802, arXiv:1104.3922.
[63] D. Hernandez, A.Y. Smirnov, arXiv:1105.5946, 2011.
[64] J.N. Bahcall, P.I. Krastev, E. Lisi, Phys. Lett. B 348 (1995) 121, hep-ph/9411414.
[65] M. Laveder, Nucl. Phys. Proc. Suppl. 168 (2007) 344, talk presented at the Workshop on Neutrino Oscillation Physics (NOW 2006), Otranto, Lecce, Italy, 9–16 September, 2006.
[66] C. Giunti, M. Laveder, Mod. Phys. Lett. A 22 (2007) 2499, hep-ph/0610352.
[67] C. Giunti, M. Laveder, Phys. Rev. D 77 (2008) 093002, arXiv:0707.4593.
[68] M.A. Acero, C. Giunti, M. Laveder, Phys. Rev. D 78 (2008) 073009, arXiv:0711.4222.
[69] C. Giunti, M. Laveder, Phys. Rev. D 80 (2009) 013005, arXiv:0902.1992.
[70] C. Giunti, M. Laveder, Phys. Rev. D 82 (2010) 053005, arXiv:1005.4599.
[71] V.N. Gavrin, V.V. Gorbachev, E.P. Veretenkin, B.T. Cleveland, arXiv:1006.2103, 2010.
[72] C. Giunti, M. Laveder, Phys. Rev. C 83 (2011) 065504, arXiv:1006.3244.
[73] S.M. Bilenky, C. Giunti, W. Grimus, Eur. Phys. J. C 1 (1998) 247, hep-ph/9607372.
[74] S.M. Bilenky, C. Giunti, W. Grimus, T. Schwetz, Phys. Rev. D 60 (1999) 073007, hep-ph/9903454.
[75] M. Maltoni, T. Schwetz, M.A. Tortola, J.W.F. Valle, Nucl. Phys. B 643 (2002) 321, hep-ph/0207157.
[76] M. Sorel, J. Conrad, M. Shaevitz, Phys. Rev. D 70 (2004) 073004, hep-ph/0305255.
[77] G. Karagiorgi, et al., Phys. Rev. D 75 (2007) 013011, hep-ph/0609177.
[78] E. Akhmedov, T. Schwetz, JHEP 1010 (2010) 115, arXiv:1007.4171.
[79] G. Karagiorgi, Z. Djurcic, J. Conrad, M.H. Shaevitz, M. Sorel, Phys. Rev. D 80 (2009) 073001, arXiv:0906.1997.
[80] J. Kopp, M. Maltoni, T. Schwetz, Phys. Rev. Lett. 107 (2011) 091801, arXiv:1103.4570.
[81] C. Giunti, M. Laveder, arXiv:1107.1452, 2011.
[82] G. Karagiorgi, DPF-2011, arXiv:1110.3735, 2011.
[83] R.E. Shrock, Phys. Lett. B 96 (1980) 159.
[84] B.H.J. McKellar, Phys. Lett. B 97 (1980) 93.
[85] I.Y. Kobzarev, B.V. Martemyanov, L.B. Okun, M.G. Shchepkin, Sov. J. Nucl. Phys. 32 (1980) 823.
[86] F. Vissani, Nucl. Phys. Proc. Suppl. 100 (2001) 273, hep-ph/0012018, Europhysics Neutrino Oscillation Workshop (NOW 2000), Conca Specchiulla, Otranto, Lecce, Italy, 9–16 September, 2000.
[87] Y. Farzan, O.L.G. Peres, A.Y. Smirnov, Nucl. Phys. B 612 (2001) 59, hep-ph/0105105.
[88] J. Studnik, M. Zralek, hep-ph/0110232, 2001.
[89] Y. Farzan, A.Y. Smirnov, Phys. Lett. B 557 (2003) 224, hep-ph/0211341.
[90] C. Kraus, et al., Eur. Phys. J. C 40 (2005) 447, hep-ex/0412056.
[91] V.M. Lobashev, Nucl. Phys. A 719 (2003) C153, 17th International Nuclear Physics Divisional Conference: Europhysics Conference on Nuclear Physics in Astrophysics (NPDC 17), Debrecen, Hungary, 30 September – 3 October 2002.
[92] F. Fraenkle, DPF-2011 Conference, Providence, RI, August 8–13, 2011, arXiv:1110.0087.
[93] C. Weinheimer, arXiv:0912.1619, 2009; International school of physics in: International School of Physics 'Enrico Fermi', CLXX Course 'Measurements of Neutrino Mass', June 17–27, 2008, Varenna, Italy.
[94] S.R. Elliott, P. Vogel, Ann. Rev. Nucl. Part. Sci. 52 (2002) 115, hep-ph/0202264.
[95] S.M. Bilenky, C. Giunti, J.A. Grifols, E. Masso, Phys. Rep. 379 (2003) 69, hep-ph/0211462.
[96] S.R. Elliott, J. Engel, J. Phys. G 30 (2004) R183, hep-ph/0405078.
[97] I. Avignone, T. Frank, S.R. Elliott, J. Engel, Rev. Mod. Phys. 80 (2008) 481, arXiv:0708.1033.
[98] W. Rodejohann, Int. J. Mod. Phys. E 20 (2011) 1833, arXiv:1106.1334.
[99] C. Giunti, Phys. Rev. D 61 (2000) 036002, hep-ph/9906275.
[100] S. Goswami, W. Rodejohann, Phys. Rev. D 73 (2006) 113003, arXiv:hep-ph/0512234.
[101] Y. Li, S. shuo Liu, arXiv:1110.5795, 2011.
[102] J. Gomez-Cadenas, J. Martin-Albo, M. Mezzetto, F. Monrabal, M. Sorel, arXiv:1109.5515, 2011.